



# Interaction investigation and phase transition of carrageenan/lysozyme complex system

Chunlan ZHANG<sup>1\*</sup>, Yuli NING<sup>2</sup>, Yin JIA<sup>2</sup>, Mengyao KANG<sup>2</sup>, Yawen HE<sup>2</sup>, Wei XU<sup>2\*</sup> , Bakht Ramin SHAH<sup>3</sup>

## Abstract

Phase transition of lysozyme/carrageenan (Ly/CRG) complex system with different ratios, pH, ionic strength and temperature conditions was explored through ultraviolet-visible spectrophotometer, fluorescence spectrophotometer, fluorescence microscope, Zeta potential. The results showed that the main force between Ly and CRG is electrostatic interaction, and the Ly/CRG composite system has undergone three phase transition states: co-solubilization, gelation and aggregation. At pH = 1-3, the oppositely charged CRG and Ly form complexes based on electrostatic interaction. Whereas at pH = 12, both CRG and Ly are negatively charged and they repel each other electrostatically. The electrostatic shielding effect of salt ions had a greater impact on the formation of Ly/CRG complex. Temperature had a certain degree of influence on the structure and turbidity of the composite system. The interaction between polysaccharides and proteins can have a significant impact on the structure and stability of complex systems and the study of polysaccharide and protein complexes which will help to expand their application in food and medicine.

**Keywords:** lysozyme;  $\kappa$ -carrageenan; ionic strength; temperature; interaction.

**Practical Application:** First, Ly/CRG soluble complex provide nano-carrier for drug and hydrophobic nutrient delivery. Addition, the interaction provide theoretical basis for selective preservation of Ly structure and activity. Finally, the phase transition condition, especially for co-solubilization, could use in regulating beverages stabilization.

## 1 Introduction

Polysaccharides and proteins, two important biological macromolecules, are also important nutrients in food (Liu et al., 2021b). Most polysaccharides and proteins belong to polyampholytes. When they are mixed in the same water environment, the state characteristics of the composite system composed of polysaccharides and proteins are related to the interaction between them (Alfaris et al., 2022; Georgilis et al., 2020; Bartlová et al., 2021). With more and more in-depth research on polysaccharide/protein complexes, we found that the interaction between polysaccharides and proteins will affect the structure and stability of the composite system (Hasizah et al., 2021; Luo et al., 2022). Among them, mutual attraction and mutual repulsion were the main interaction modes, and they were affected by factors such as the composite ratio, pH, ionic strength, and temperature of the composite system (Xu et al., 2020). When polysaccharides and proteins have opposite charges, under the action of static electricity, they can form a homogeneous soluble complex or form an insoluble complex system (Jiang et al., 2022), which will cause phase separation. When a protein is positively charged and forms a complex system with a negatively charged polysaccharide, especially when the pH of the system is between the electrolyte constant of the polysaccharide and the isoelectric point of the protein, they will interact strongly to form a complex.

Carrageenan (CRG) is a naturally occurring sulphated polysaccharide derived from red seaweed and extracted from red seaweed (Yang et al., 2020), it is used as a thickener, stabilizer and texturizing agent in the food industry (Huang et al., 2021; Jancikova et al., 2020). CRG can form a translucent or transparent flowable colloidal solution with a certain viscosity, which is affected by pH, temperature and ion concentration. CRG is widely used as a food additive and fat substitute in the food industry and is commonly used for ice cream, yoghurt, whipped cream and cheese due to its special thickening, foaming, emulsifying and gelling abilities (Liu et al., 2021a).

Lysozyme (Ly) is widely present in mammalian blood, milk, saliva and various tissues (How et al., 2019). The relative molecular mass of Ly is about 14000, and it often exists as a white or slightly white freeze-dried powder. It is soluble in water but not soluble in organic solvents such as ether and acetone. Ly can exist stably under acidic conditions but is easily inactivated under alkaline conditions. Ly can destroy or kill bacteria by hydrolyzing the  $\beta$ -1,4-bond in the bacterial cell wall. Ly from egg whites is a natural protein with bactericidal activity and is widely used in the food industry against gram-positive bacteria (Wang et al., 2021; Li et al., 2021). Nowadays, Ly has been widely used in the fields of food processing and medicine. It can be added to

Received 21 July, 2022

Accepted 27 September, 2022

<sup>1</sup>College of Food Science and Engineering, Tarim University, Alar, China

<sup>2</sup>College of Life Science, Xinyang Normal University, Xinyang, China

<sup>3</sup>South Bohemian Research Center of Aquaculture and Biodiversity of Hydrocenoses, Faculty of Fisheries and Protection of Waters, Institute of Aquaculture and Protection of Waters, University of South Bohemia in České Budějovice, České Budějovice, Czech Republic

\*Corresponding author: zcl790225@163.com; toxuwei1986@163.com; xuwei@xynu.edu.cn

meat products, aquatic products, cakes and beverages to play a preservative effect (Beaussart et al., 2021; Sarkar et al., 2020).

The interaction between proteins and polysaccharides has attracted a lot of attention, they can be used as emulsion stabilizers, fat substitutes and encapsulation of nutrients (Ashaolu & Zhao, 2020; Zhang et al., 2021b). The different composite ratios of proteins and polysaccharides, the pH of the solution, ionic strength and temperature are the main factors affecting the electrostatic interaction between the composite system. Under different conditions, the combination of them will undergo a change of conformational and degree of stability (Huang et al., 2021; Xu et al., 2022).

In this paper, the effects of solution pH, ionic strength and temperature, on the light transmission, potential value and microscopic morphology of the Ly/CRG complex system were investigated to provide the corresponding theoretical basis and reference materials for future preparation, application and research of CRG/Ly complexes in the food and pharmaceutical fields.

## 2 Materials and methods

### 2.1 Materials

Lysozyme (Ly, 14.3 kDa) from chicken egg white, was purchased from National Medicine Group Chemical Reagent Co., Ltd.  $\kappa$ -Carrageenan (CRG,  $5 \times 10^5$  Da, 90% (w/w)) was obtained from Aladdin Chemistry Co., Ltd. Other chemicals were reagent grade and used without purification. All the solutions used in the experiments were prepared using ultrapure water through a Millipore (Millipore, Milford, MA, USA) Milli-Q water purification system.

### 2.2 Preparation of Ly/CRG complex

Ly and CRG samples were accurately weighed and then slowly added to a certain amount of ultrapure water to prepare a final concentration of 1 mg/mL of Ly and CRG solution. Finally, Ly and CRG were prepared to different ratios of the composite system. The initial pH of Ly mother liquor was adjusted to 7.0 at room temperature and stirred for 1 hour to remove impurities. The CRG solution was stirred at 70 °C for 20 minutes and then naturally cooled to room temperature and filtered to remove impurities. The initial pH was also adjusted to 7.0. At room temperature, Ly/CRG compound solutions were prepared by mixing Ly and CRG in different volume ratios. The CRG solution was added to the mother liquor of Ly and the Ly/CRG complex was prepared by stirring for 10 min to mix the mixture well.

### 2.3 Light transmission of Ly/CRG complex

At room temperature, the light transmittance of different Ly/CRG composite systems was measured at 600 nm with a UV spectrophotometer (Dang et al., 2018), and each group of samples was measured twice. The changes in light transmission T% of Ly/CRG complexes were then also observed and compared at different pH values (pH = 1-12), different ionic strengths (0 mM-120 mM), different temperatures (25 °C, 40 °C, 60 °C, 80 °C), at different ratios (1:7, 1:3, 1:2, 1:1, 2:1) and different temperature conditions (25 °C, 40 °C, 60 °C, 80 °C) separately.

### 2.4 Ultraviolet visible spectra of Ly/CRG complex

The ultraviolet-visible spectra of different ratios of Ly/CRG (1:2, 1:3, 1:5 and 1:7) at 250-500 nm were measured three times using an ultraviolet-visible photometer. The same concentrations of Ly solution were used as controls.

### 2.5 Fluorescence spectra of Ly/CRG complex

Different Ly/CRG complex ratios (1:7, 1:5, 1:3, 1:2) were prepared at room temperature, while same concentrations of Ly solution were used as controls. Using a fluorescence spectrometer (Zhang et al., 2021b), adjusted to a fixed excitation wavelength  $\lambda_{ex}$  of 280 nm, excitation and emission slit width were 2.5 nm and 2.5 nm, voltage 400 V, spectral scanning speed of 60 nm/min, set the scan range 290-500 nm, fluorescence spectra were obtained in different proportions. Furthermore, Ly and CRG were prepared in different ratios (2:1, 1:2, 1:3, 1:7), the system temperature was adjusted and incubated at different conditions (25 °C, 40 °C, 60 °C, 80 °C) and the fluorescence spectra were then measured.

### 2.6 $\zeta$ potential of Ly/CRG complex

The surface charges of different ratios of Ly/CRG composite systems (1:7, 1:5, 1:3, 1:2, 1:1, 2:1, 3:1) were determined using a  $\zeta$ -potentiometer. The electrophoretic mobility of the relationship between UE and zeta potential satisfies the Henry equation (Miliaieva et al., 2021) (Equation 1):

$$\xi = \frac{3\eta UE}{2\epsilon f(Ka)} \quad (1)$$

$\zeta$  is representative of the viscosity of the solution,  $\epsilon$  represents the dielectric constant of the solvent, UE represents the electrophoretic mobility,  $f(Ka)$  represents the Henry constant.

### 2.7 Fluorescence microscope of Ly/CRG complex

The Ly/CRG (2:1) composite solution was prepared and 0.2% rhodamine B fluorescent dye (used to label Ly) was added to it for 15  $\mu$ L, and the sample was well mixed using a magnetic stirrer. A drop of the solution was then gently placed on a slide to ensure no air bubbles were produced. Followed by a coverslip and placed under a fluorescence microscope to observe the phase transition microstructure morphology of the Ly/CRG composite system.

## 3 Results and discussion

### 3.1 Light transmittance of Ly/CRG systems at different ratios

The light transmission of the systems reflects the differences in the aggregation and stability of Ly and CRG in the composite system. As shown in Figure 1, with the increasing proportion of Ly and decreasing proportion of CRG, the transmittance of the composite system gradually decreased. The solution transmittance was strongest when the ratio of Ly/CRG is 1:9. The transmittance changed slowly and steadily between Ly/CRG ratio from 1:9 to 1:5, after which the transmittance decreased sharply. The composite

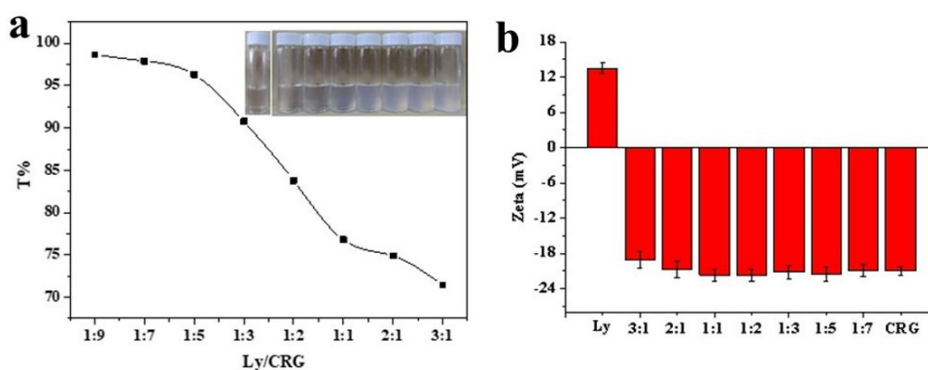


**Figure 1.** Transmittance (a) and  $\zeta$ -potential (b) of Ly/CRG complex with different ratios.

system gradually changed from clarification to translucency until a little white precipitate appeared.

The higher the proportion of Ly, the lower the light transmittance seeing as the figure, which indicated that Ly can promote the phase transformation process of Ly/CRG system. In the case of lysozyme carrageenan 1:9, the complex solutions were transparent at pH 7, which indicates that they didn't form particles large enough to strongly scatter light, because the CRG sulfate group was always ionized, giving the molecules an electrostatic repulsive force (Antonov & Zhuravleva, 2019).

### 3.2 $\zeta$ -potential of Ly/CRG systems at different ratios

In a certain electric field, the charged colloidal particles in the Ly/CRG system will be migrated, and the charging status of the system can be reflected by its  $\zeta$ -potential (mV), which can reflect the stability of its dispersion solution. Z-potential is an important factor affecting the stability of the Ly/CRG composite system, and it mainly affects the repulsive potential of the solution in the system. As the  $\zeta$  potential increases, the repulsive potential energy of the solution will increase, and the energy needed to overcome the thermal motion of the molecules will also increase. Thus the composite system will become more stable (Huang et al., 2019).

As shown in Figure 1b, the  $\zeta$  potentials of the Ly/CRG composite system under different composite ratios were shown. Ly was partially positively charged, and the potential was about 14 mV. While CRG was partially negatively charged, and the potential was about -21 mV. As the content of CRG increases, the dissociation of its carboxyl group made it more negatively charged. The positive charge of Ly was gradually neutralized by the added CRG, so the amount of negative charge carried by the Ly/CRG composite system gradually increases. The total negative charge in the system tended to be stable until the Ly/CRG ratio is 1:3 (Yang et al., 2021).

### 3.3 Ultraviolet visible spectrum of Ly/CRG systems at different ratios

It can be seen from Figure 2 that the composite system had a peak at a wavelength of about 285 nm. The UV absorption peak was significantly reduced in the Ly/CRG composite system after adding CRG. This result was consistent with the phenomenon

in fluorescence spectra. This may be because the electrostatic interaction forces between the complexes composed of Ly and CRG alter the spatial structural arrangement of the atoms and molecules in the complexes. And through comprehensive comparison, as the proportion of Ly continues to rise, the absorption peak of the Ly/CRG composite system showed a gradually decreasing trend. Due to the structural change of the composite, the material had a significant decline under the conditions of 1:3 and 1:5.

### 3.4 Fluorescence spectra of Ly/CRG systems at different ratios

The composite system had a peak at a wavelength of about 340nm as shown in Figure 3. The fluorescence spectrum peaks in the Ly/CRG composite system after adding CRG had a significant decrease. The wavelength of maximum emission ( $\lambda_{max}$ ) for Ly is about 340 nm. This fluorescence peak exclusively arises from the tryptophan residues of Ly. When different amounts of CRG were dropped onto a fixed concentration of Ly, the fluorescence intensity of Ly decreased and the position of the fluorescence peak did not change significantly. This may be due to static quenching caused by the formation of CRG/Ly complexes (Antonov et al., 2018; Walker et al., 2019). And through comprehensive comparison, it can be found that as the proportion of Ly decreases, the peak value of the fluorescence spectrum has also changed. In Figure 3a, the peak value was 90. In Figure 3b, c, the peak values were basically around 110, while it changed to 100 in Figure 3d. The degree of system composite was the highest, and the interaction between them was the strongest when the ratio of Ly/CRG complex was 1:3 and 1:5.

### 3.5 Light transmittance of Ly/CRG complex system at different pH values

Since Ly is a protein, its secondary structure conformation mainly includes  $\alpha$ -helix,  $\beta$ -sheet,  $\beta$ -turn and random coils. The main function of stabilizing its secondary structure is hydrogen bonding. Ly and CRG formed their Ly/CRG complex through electrostatic interaction. When the pH value was low, because Ly was partially positively charged, the repulsive force between the Ly/CRG composite system was weak, and there was a strong electrostatic attraction between them. And due to the low potential, the system was not very stable, so that a

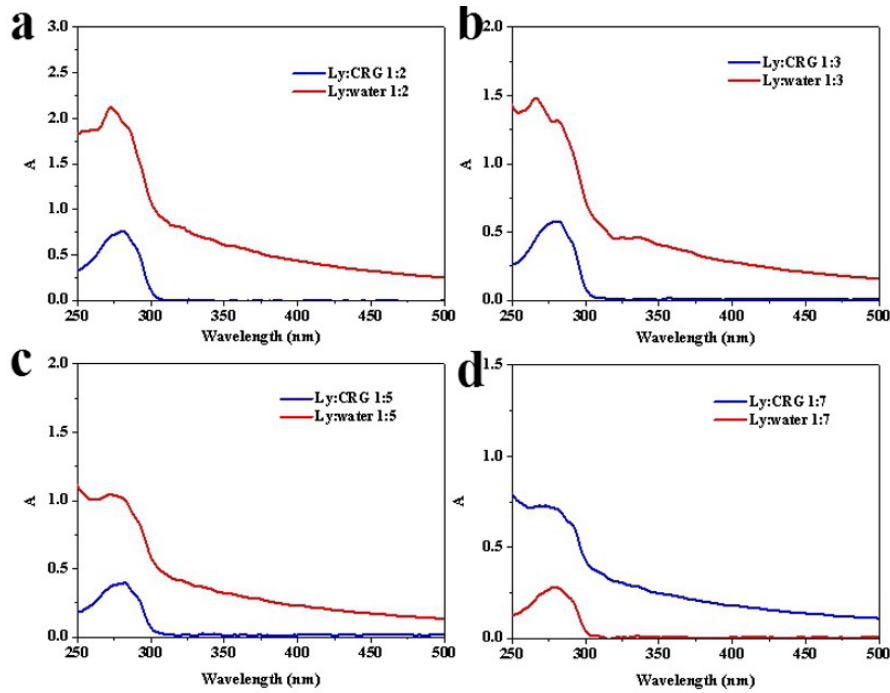


Figure 2. Ultraviolet visible spectrum of Ly/CRG complex with different ratios (a 1:2, b 1:3, c 1:5, d 1:7).

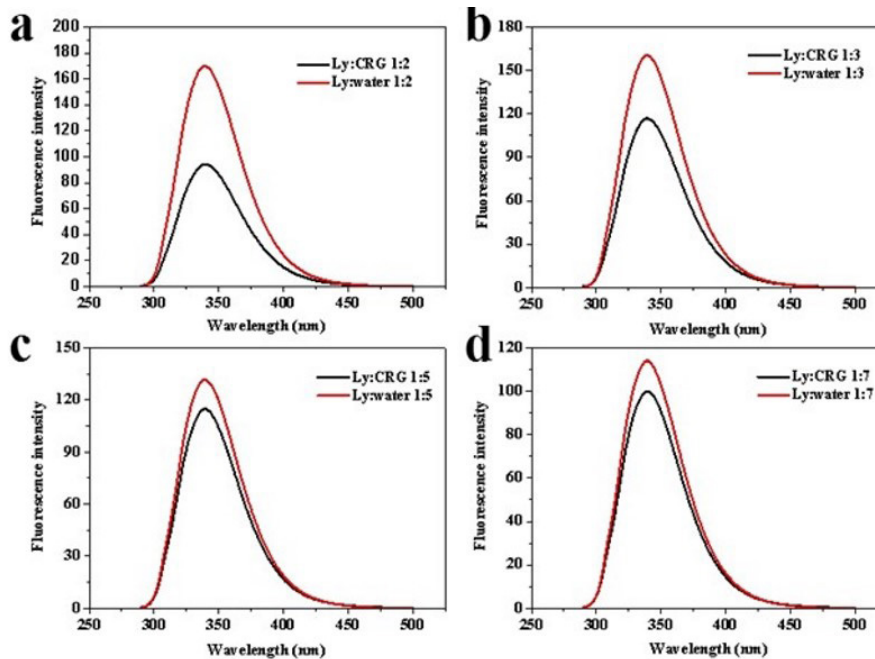
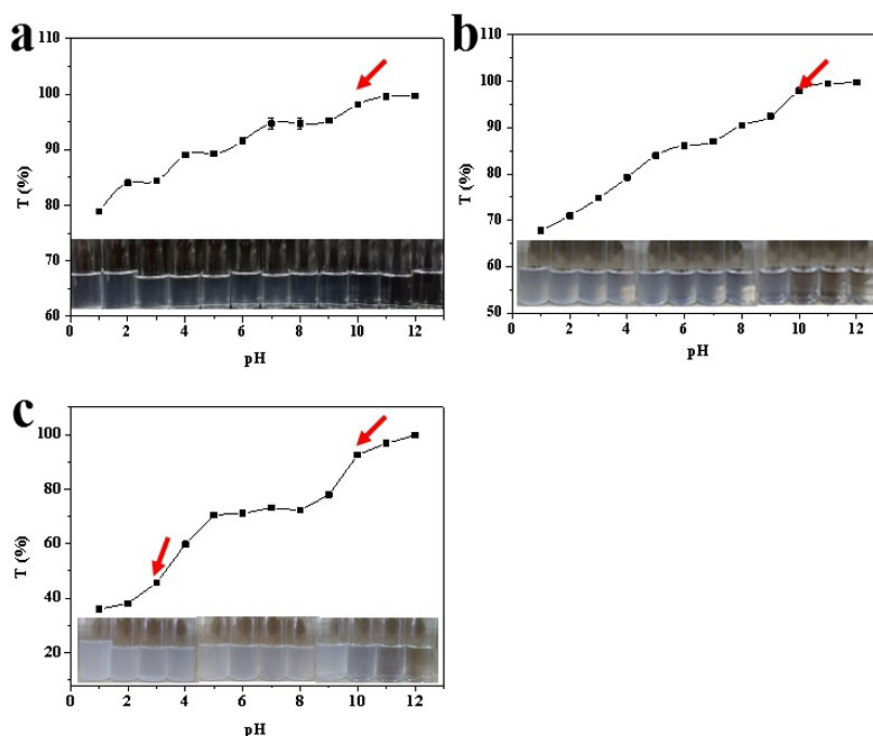


Figure 3. Fluorescence spectra of Ly/CRG complex with different ratios (a 1:2, b 1:3, c 1:5, d 1:7).

large range of aggregation occurred to form a white insoluble complex and precipitate (Seo et al., 2018). As the pH of the system increased, both Ly and CRG were partially negatively charged and the carboxyl group of CRG was protonated. The mutual attraction between the two was greatly weakened, as well as the strong repulsive forces between Ly and CRG arose, leading to the dissociation of the complexes (Zhang et al., 2021a).

As the ratio of Ly/CRG composite system increased, the system gradually changes from clarification to turbidity until white insoluble substances were produced seeing as Figure 4. The composite system had a slight blue opalescence phenomenon in Figure 4b, resulting in a light blue colloidal compound. Due to the increasing proportion of Ly and the decreasing proportion of CRG, CRG polysaccharide molecules were introduced into



**Figure 4.** Light transmittance of Ly/CRG complex at different pH conditions (a 1:7, b 1:3, c 1:1).

the peptide chains of Ly in the composite system. The steric hindrance of its polysaccharide chain made the content of alpha helix increase, the content of random coil decrease. Hence the secondary structure of Ly was changed and the order of its structure was enhanced. After adding CRG, the electrostatic interaction between Ly molecules and the molecular conformation of Ly/CRG had been affected, and the Ly/CRG complex was formed.

### 3.6 Light transmittance of Ly/CRG system under different ionic strength

As shown in Figure 5a, when the NaCl solution was not added, as the Ly/CRG composite ratio increased, the light transmittance of the composite system gradually decreased from the clear state (light transmittance 97%). After the Ly/CRG ratio of 1:2, the decrease was obvious and the turbidity increased. When the ion concentration of the NaCl solution was 10mM, the composite system had a high light transmittance. Then the light transmittance of the Ly/CRG composite gradually decreased and finally stabilized as the salt ion concentration increased. The shielding effect of salt ions on the charge was an important factor affecting the interaction between Ly and CRG (Brudar & Hribar-Lee, 2019). Due to the addition of NaCl solution, the ionic strength of the composite system was increased. As a result, the surface charge effect of Ly and CRG was shielded, the electrostatic interaction between Ly and CRG was inhibited. At low ionic strength, the competitive adsorption capacity of  $\text{Na}^+$  and  $\text{Cl}^-$  was weak, and the degree of interaction between Ly and CRG was also low. When the concentration of NaCl gradually increases,  $\text{Na}^+$  binds to the negative charge on the polysaccharide chain and competes with the positive charge

binding site of Ly, and  $\text{Cl}^-$  bound to the positive charge on Ly and competed with the negative charge binding site on the CRG chain. Therefore, the force between Ly and CRG was weakened, which was not conducive to the formation of Ly/CRG complex. The presence of salt ions had a certain electrostatic shielding effect on the formation of complexes (Yu et al., 2022). It also shows that Ly and CRG were mainly composed of a composite system formed by electrostatic interaction.

### 3.7 Light transmittance of different ratios of Ly/CRG complex after heat treatment

The light transmission of the composite system gradually decreases from close to 100% until a white insoluble composite appears in Figure 5b. This was consistent with the results in Figure 1, probably because the CRG molecule carries electrostatic repulsion and Ly and CRG do not form a stable complex (Liu et al., 2021a). While under a specific compounding ratio, as the temperature of the system rose, its light transmittance also tended to decrease slightly. This is probably since heating has changed the molecular structure of Ly.

### 3.8 Heating phase transition of Ly/CRG systems at different ratios

With the increase of the Ly/CRG composite ratio, the light transmittance gradually decreased from the clear state (light transmittance 97%) as shown in Figure 5c-5d, and a light blue opalescent colloidal compound would be produced in the middle. Then the turbidity of the composite system increased, and white insoluble composites appear. As the proportion of

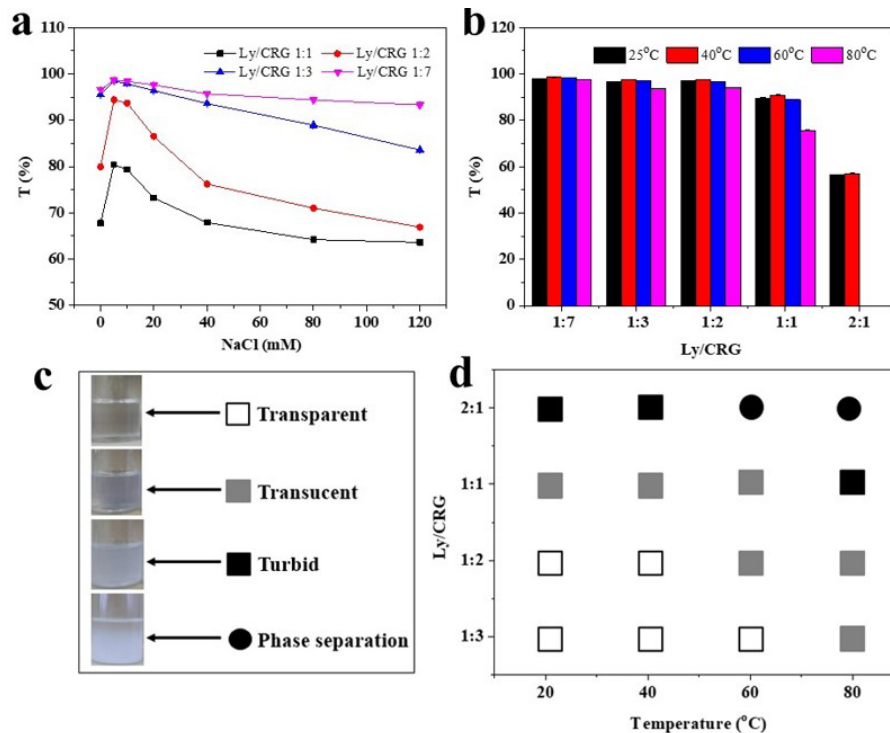


**Figure 5.** Light transmittance and of Ly/CRG complex with different ionic strengths (a) and heat treatment (b), and phase transition (c, d) of Ly/CRG complex systems after heat treatment (c, pictures of morphological observations, d heated phase transitions at different temperatures).

CRG increased, the more clarified the composite system was, and the less likely to produce white aggregates. This indicates that the system was more stable with a larger amount of CRG, which was related to the fact that CRG had a certain higher viscosity (Liu et al., 2021a). And under a certain composite ratio, as the reaction temperature conditions increased, the composite gradually changes from a transparent state to a semi-opaque state, until white precipitates were produced. This may be since heating at high temperatures exposed the hydrophobic amino acid residues inside the lysozyme, leading to an increase in hydrophobicity on its surface. It also increased the interaction between protein molecules through hydrophobic interactions, leading to aggregation, which was detrimental to the stability of the system.

### 3.9 Fluorescence spectra after heating of Ly/CRG composite system at different ratios

The Ly/CRG composite system had a peak at a wavelength of about 340 nm seeing as Figure 6. As the temperature of the system increased, the fluorescence spectrum peaks significantly decreased, which led to corresponding changes in the composite system. This was because heating caused greater changes in the secondary structure of Ly, and the hydrophobic interaction inhibited the formation of Ly/CRG complexes to a weaker extent (Magsumov et al., 2019). As the temperature increased, the content of  $\alpha$ -helix in Ly decreased, and the content of random coils increased. The rise in temperature accelerates the movement of molecules in the system, and the hydrophobic interaction

between molecules was enhanced. Ly was thermally denatured due to the influence of temperature, and its internal hydrogen bonds were destroyed, and its peptide chain was stretched by heat so that the molecular space structure was unfolded (Wu et al., 2020). CRG and Ly formed soluble complexes as a result of electrostatic interactions. It was conducive to the stability of Ly's secondary structure, thereby increasing the degree of stability to heat, and inhibiting the occurrence of aggregation (Guo et al., 2021).

### 3.10 Phase transition micro morphology of Ly/CRG composite system

The Ly/CRG composite solution was prepared in proportion and placed under a fluorescent microscope to observe the phase change microstructure morphology of the Ly/CRG composite system. As can be seen in Figure 6, the agglomeration of the composite system deepens and the phase separation increases in the Ly/CRG composite system. Small particles aggregated into large particles, and the molecular size of the particles increased accordingly. Because under higher temperature conditions, Ly was affected by high temperature, which led to changes in molecular structure (Bao et al., 2018). Then the Ly/CRG composite system aggregated due to instability and caused phase separation. Under the condition of a higher Ly/CRG ratio, as the temperature increased, more Ly bound to the polysaccharide chain of CRG, and the degree of aggregation of the system became larger so that large particles are formed (Omar et al., 2020).

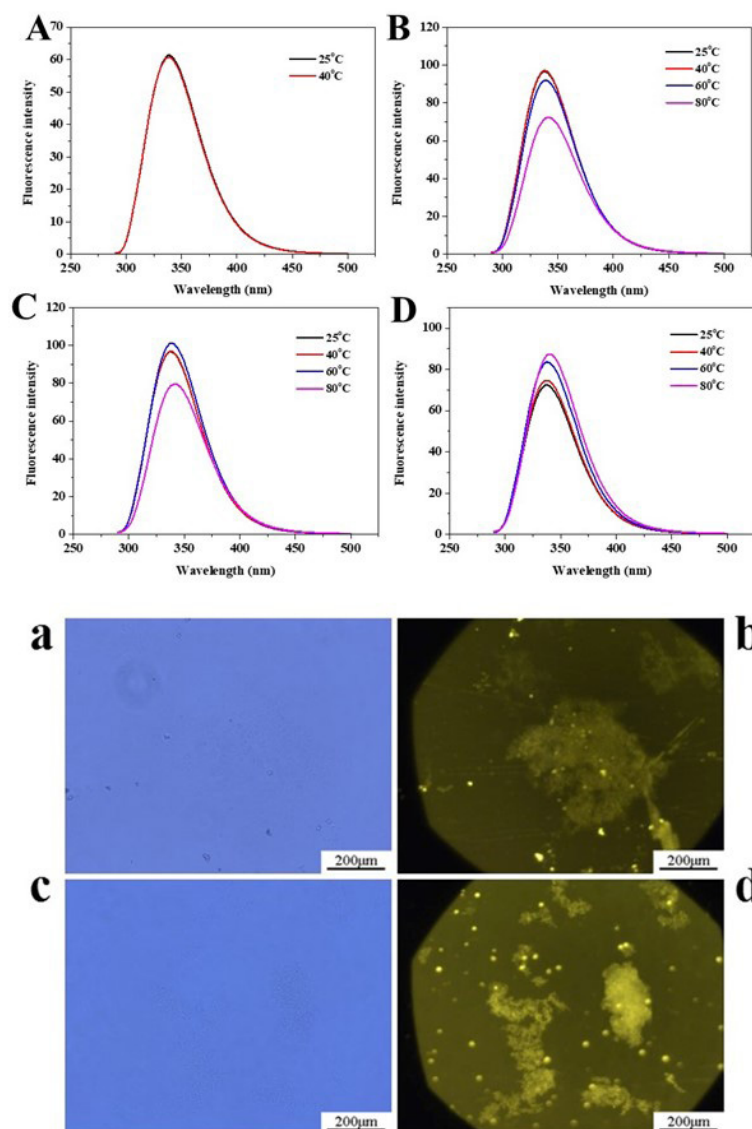


**Figure 6.** Fluorescence spectra (A, B, C, D) and micromorphology (a, b, c, d) of Ly/CRG complex after heat treatment (a, b, 60 °C and c, d 80 °C) with different ratios (A 2:1, B 1:2, C 1:3, D 1:7). Bright field, a and c; fluorescent images, b and d.

#### 4 Conclusion

This study showed that the main force between Ly and CRG is electrostatic interaction. The Ly/CRG composite system has undergone three phase transition states: co-solubilization, gelation and aggregation. The oppositely charged CRG and Ly form complexes based on electrostatic interaction at pH 1-3. Whereas at pH 12, both CRG and Ly are negatively charged and they repel each other electrostatically. The electrostatic shielding effect of salt ions had a greater impact on the formation of Ly/CRG complex. Temperature had a certain degree of influence on the structure and turbidity of the composite system. The interaction between polysaccharides and proteins could provide theoretical basis on regulation on the structure and stability of food.

#### Ethical approval

There is no ethics interest related in research.

#### Conflict of interest

There is no professional or other personal interest of any service and/or company that could be construed as influencing the position presented in the manuscript. The work has not been published before. No conflict of interest exists in the submission of this manuscript.

#### Author contributions

All the authors listed have participated the research and approved the manuscript that is enclosed.

#### References

Alfaris, N. A., Gupta, A. K., Khan, D., Khan, M., Wabaidur, S. M., Altamimi, J. Z., Alothman, Z. A., & Aldayel, T. S. (2022). Impacts of wheat bran on the structure of the gluten network as studied

- through the production of dough and factors affecting gluten network. *Food Science and Technology*, 42, e37021. <http://dx.doi.org/10.1590/fst.37021>.
- Antonov, Y. A., & Zhuravleva, I. L. (2019). Complexation of lysozyme with lambda carrageenan: complex characterization and protein stability. *Food Hydrocolloids*, 87, 519-529. <http://dx.doi.org/10.1016/j.foodhyd.2018.08.040>.
- Antonov, Y. A., Zhuravleva, I. L., Cardinaels, R., & Moldenaers, P. (2018). Macromolecular complexes of lysozyme with kappa carrageenan. *Food Hydrocolloids*, 74, 227-238. <http://dx.doi.org/10.1016/j.foodhyd.2017.07.022>.
- Ashaolu, T. J., & Zhao, G. (2020). Fabricating a pickering stabilizer from okara dietary fibre particulates by conjugating with soy protein isolate via Maillard reaction. *Foods*, 9(2), 143. <http://dx.doi.org/10.3390/foods9020143>. PMID:32024017.
- Bao, W., Li, Q., Wu, Y., & Ouyang, J. (2018). Insights into the crystallinity and in vitro digestibility of chestnut starch during thermal processing. *Food Chemistry*, 269, 244-251. <http://dx.doi.org/10.1016/j.foodchem.2018.06.128>. PMID:30100431.
- Bartlová, M., Ziólkowska, D., Pospiech, M., Shyichuk, A., & Tremlová, B. (2021). Determination of carrageenan in jellies with new methylene blue dye using spectrophotometry, smartphone-based colorimetry and spectrophotometric titration. *Food Science and Technology*, 41(Suppl. 1), 81-90. <http://dx.doi.org/10.1590/fst.01220>.
- Beaussart, A., Retourney, C., Quilès, F., Morais, R. S., Gaiani, C., Fiérobe, H.-P., & El-Kirat-Chatel, S. (2021). Supported lysozyme for improved antimicrobial surface protection. *Journal of Colloid and Interface Science*, 582(Pt B), 764-772. <http://dx.doi.org/10.1016/j.jcis.2020.08.107>. PMID:32916574.
- Brudar, S., & Hribar-Lee, B. (2019). The role of buffers in wild-type HEWL amyloid fibril formation mechanism. *Biomolecules*, 9(2), 65. <http://dx.doi.org/10.3390/biom9020065>. PMID:30769878.
- Dang, Q., Liu, K., Liu, C., Xu, T., Yan, J., Yan, F., Cha, D., Zhang, Q., & Cao, Y. (2018). Preparation, characterization, and evaluation of 3, 6-ON-acetylenediamine modified chitosan as potential antimicrobial wound dressing material. *Carbohydrate Polymers*, 180, 1-12. <http://dx.doi.org/10.1016/j.carbpol.2017.10.019>. PMID:29103484.
- Georgilis, E., Abdelghani, M., Pille, J., Aydinlioglu, E., van Hest, J. C. M., Lecommandoux, S., & Garanger, E. (2020). Nanoparticles based on natural, engineered or synthetic proteins and polypeptides for drug delivery applications. *International Journal of Pharmaceutics*, 586, 119537. <http://dx.doi.org/10.1016/j.ijpharm.2020.119537>. PMID:32531450.
- Guo, Z., Liu, M., Xiang, X., Wang, Z., Yang, B., Chen, X., Chen, G., & Kan, J. (2021). Effects of inulins with various molecular weights and added concentrations on the structural properties and thermal stability of heat-induced gliadin and glutenin gels. *Lebensmittel-Wissenschaft + Technologie*, 149, 111891. <http://dx.doi.org/10.1016/j.lwt.2021.111891>.
- Hasizah, A., Mahendradatta, M., Laga, A., Metusalach, M., & Salengke, S. (2021). Extraction of carrageenan from *Eucheuma spinosum* using ohmic heating: optimization of extraction conditions using response surface methodology. *Food Science and Technology*, 41(4), 928-937. <http://dx.doi.org/10.1590/fst.26220>.
- How, S. C., Hsin, A., Chen, G. Y., Hsu, W. T., Yang, S. M., Chou, W. L., Chou, S. H., & Wang, S. S. S. (2019). Exploring the influence of brilliant blue G on amyloid fibril formation of lysozyme. *International Journal of Biological Macromolecules*, 138, 37-48. <http://dx.doi.org/10.1016/j.ijbiomac.2019.07.055>. PMID:31295491.
- Huang, L., Cai, Y., Liu, T., Zhao, X., Chen, B., Long, Z., Zhao, M., Deng, X., & Zhao, Q. (2019). Stability of emulsion stabilized by low-concentration soybean protein isolate: effects of insoluble soybean fiber. *Food Hydrocolloids*, 97, 105232. <http://dx.doi.org/10.1016/j.foodhyd.2019.105232>.
- Huang, M., Mao, Y., Li, H., & Yang, H. (2021). Kappa-carrageenan enhances the gelation and structural changes of egg yolk via electrostatic interactions with yolk protein. *Food Chemistry*, 360, 129972. <http://dx.doi.org/10.1016/j.foodchem.2021.129972>. PMID:33971508.
- Jancikova, S., Dordevic, D., Jamroz, E., Behalova, H., & Tremlova, B. (2020). Chemical and physical characteristics of edible films, based on kappa- and lambda-carrageenans with the addition of lapacho tea extract. *Foods*, 9(3), 357. <http://dx.doi.org/10.3390/foods9030357>. PMID:32204468.
- Jiang, F., Pan, Y., Peng, D., Huang, W., Shen, W., Jin, W., & Huang, Q. (2022). Tunable self-assemblies of whey protein isolate fibrils for pickering emulsions structure regulation. *Food Hydrocolloids*, 124, 107264. <http://dx.doi.org/10.1016/j.foodhyd.2021.107264>.
- Li, H., Chen, Y., Tang, H., Zhang, J., Zhang, L., Yang, X., Wang, F., & Chen, L. (2021). Effect of lysozyme and Chinese liquor on *Staphylococcus aureus* growth, microbiome, flavor profile, and the quality of dry fermented sausage. *Lebensmittel-Wissenschaft + Technologie*, 150, 112059. <http://dx.doi.org/10.1016/j.lwt.2021.112059>.
- Liu, B., Zhu, S., Zhong, F., Yokoyama, W., Huang, D., & Li, Y. (2021a). Modulating storage stability of binary gel by adjusting the ratios of starch and kappa-carrageenan. *Carbohydrate Polymers*, 268, 118264. <http://dx.doi.org/10.1016/j.carbpol.2021.118264>. PMID:34127213.
- Liu, K., Chen, Y. Y., Zha, X. Q., Li, Q. M., Pan, L. H., & Luo, J. P. (2021b). Research progress on polysaccharide/protein hydrogels: preparation method, functional property and application as delivery systems for bioactive ingredients. *Food Research International*, 147, 110542. <http://dx.doi.org/10.1016/j.foodres.2021.110542>. PMID:34399519.
- Luo, W., Liu, F., Qi, X., & Dong, G. (2022). Research progress of konjac dietary fibre in the prevention and treatment of diabetes. *Food Science and Technology*, 42, e23322. <http://dx.doi.org/10.1590/fst.23322>.
- Magsumov, T., Fatkhutdinova, A., Mukhametzyanov, T., & Sedov, I. (2019). The effect of dimethyl sulfoxide on the lysozyme unfolding kinetics, thermodynamics, and mechanism. *Biomolecules*, 9(10), 547. <http://dx.doi.org/10.3390/biom9100547>. PMID:31569484.
- Miliaieva, D., Matunova, P., Cermak, J., Stehlik, S., Cernescu, A., Remes, Z., Stenclova, P., Muller, M., & Rezek, B. (2021). Nanodiamond surface chemistry controls assembly of polypyrrole and generation of photovoltage. *Scientific Reports*, 11(1), 590. <http://dx.doi.org/10.1038/s41598-020-80438-3>. PMID:33437005.
- Omar, A. M., Elfaky, M. A., Arold, S. T., Soror, S. H., Khayat, M. T., Asfour, H. Z., Bamane, F. H., & El-Araby, M. E. (2020). 1H-imidazole-2,5-dicarboxamides as NS4A peptidomimetics: identification of a new approach to inhibit HCV-NS3 protease. *Biomolecules*, 10(3), 479. <http://dx.doi.org/10.3390/biom10030479>. PMID:32245218.
- Sarkar, S., Gulati, K., Mishra, A., & Poluri, K. M. (2020). Protein nanocomposites: special inferences to lysozyme based nanomaterials. *International Journal of Biological Macromolecules*, 151, 467-482. <http://dx.doi.org/10.1016/j.ijbiomac.2020.02.179>. PMID:32084483.
- Seo, S., Perez, G. A., Tewari, K., Comas, X., & Kim, M. (2018). Catalytic activity of nickel nanoparticles stabilized by adsorbing polymers for enhanced carbon sequestration. *Scientific Reports*, 8(1), 11786. <http://dx.doi.org/10.1038/s41598-018-29605-1>. PMID:30082729.
- Walker, E. J., Bettinger, J. Q., Welle, K. A., Hryhorenko, J. R., & Ghaemmaghami, S. (2019). Global analysis of methionine oxidation provides a census of folding stabilities for the human proteome. *Proceedings of the National Academy of Sciences of the United States of America*, 116(13), 6081-6090. <http://dx.doi.org/10.1073/pnas.1819851116>. PMID:30846556.

- Wang, Y., Xue, Y., Bi, Q., Qin, D., Du, Q., & Jin, P. (2021). Enhanced antibacterial activity of eugenol-entrapped casein nanoparticles amended with lysozyme against gram-positive pathogens. *Food Chemistry*, 360, 130036. <http://dx.doi.org/10.1016/j.foodchem.2021.130036>. PMID:34004594.
- Wu, D., Tu, M., Wang, Z., Wu, C., Yu, C., Battino, M., El-Seedi, H. R., & Du, M. (2020). Biological and conventional food processing modifications on food proteins: structure, functionality, and bioactivity. *Biotechnology Advances*, 40, 107491. <http://dx.doi.org/10.1016/j.biotechadv.2019.107491>. PMID:31756373.
- Xu, W., Li, Z., Sun, H., Zheng, S., Li, H., Luo, D., Li, Y., Wang, M., & Wang, Y. (2022). High internal-phase pickering emulsions stabilized by xanthan gum/lysozyme nanoparticles: rheological and microstructural perspective. *Frontiers in Nutrition*, 8, 744234. <http://dx.doi.org/10.3389/fnut.2021.744234>. PMID:35071292.
- Xu, W., Xiong, Y., Li, Z., Luo, D., Wang, Z., Sun, Y., & Shah, B. R. (2020). Stability, microstructural and rheological properties of complex prebiotic emulsion stabilized by sodium caseinate with inulin and konjac glucomannan. *Food Hydrocolloids*, 105, 105772. <http://dx.doi.org/10.1016/j.foodhyd.2020.105772>.
- Yang, D., Gao, S., & Yang, H. (2020). Effects of sucrose addition on the rheology and structure of iota-carrageenan. *Food Hydrocolloids*, 99, 105317. <http://dx.doi.org/10.1016/j.foodhyd.2019.105317>.
- Yang, F., Yang, J., Qiu, S., Xu, W., & Wang, Y. (2021). Tannic acid enhanced the physical and oxidative stability of chitin particles stabilized oil in water emulsion. *Food Chemistry*, 346, 128762. <http://dx.doi.org/10.1016/j.foodchem.2020.128762>. PMID:33385917.
- Yu, J., Wang, Y., Li, D., & Wang, L. J. (2022). Freeze-thaw stability and rheological properties of soy protein isolate emulsion gels induced by NaCl. *Food Hydrocolloids*, 123, 107113. <http://dx.doi.org/10.1016/j.foodhyd.2021.107113>.
- Zhang, X., Lei, Y., Luo, X., Wang, Y., Li, Y., Li, B., & Liu, S. (2021a). Impact of pH on the interaction between soybean protein isolate and oxidized bacterial cellulose at oil-water interface: dilatational rheological and emulsifying properties. *Food Hydrocolloids*, 115, 106609. <http://dx.doi.org/10.1016/j.foodhyd.2021.106609>.
- Zhang, Y., Lin, L., Cui, H., Li, B., & Tian, J. (2021b). Construction and application of EGCG-loaded lysozyme/pectin nanoparticles for enhancing the resistance of nematodes to heat and oxidation stresses. *Foods*, 10(5), 1127. <http://dx.doi.org/10.3390/foods10051127>. PMID:34069528.